Fuzzy Sets and Systems 48 (1992) 23–40
North-Holland


# Fuzzy geometry in image analysis

Sankar K. Pal* and Ashish Ghosh
*Electronics & Communication Sciences Unit, Indian Statistical Institute, 203 Barrackpore Trunk Road, Calcutta 700035, India*

Received August 1989
Revised October 1990

*Abstract:* An attempt is made here to demonstrate the way of implementing the concept of fuzzy geometry in image processing/analysis problems. Some new measures are also provided in this context. Four algorithms are described for object/background classification and skeleton extraction in both fuzzy and nonfuzzy (crisp) forms. Their effectiveness is demonstrated on various types of images. The crisp (nonfuzzy) outputs of the proposed algorithms are compared with the results of some of the recently developed conventional techniques.

*Keywords:* Fuzzy geometry; gray level thresholding; pixel classification; skeletonization.

## 1. Introduction

The conventional approach to image analysis/recognition/interpretation consists of segmenting the image into meaningful regions, extracting its different features (e.g. edges, skeletons) and computing the various properties of and relationships among the regions. However the regions in an image are not always crisply defined and it becomes sometimes more convenient and appropriate to regard them as fuzzy subsets of the image [10, 14], the subsets being characterized by the possibility (degree) of belongingness of each pixel to them. There is a great deal of work in this regard by Rosenfeld [11–17] who generalized many standard geometric properties of and relations among regions in an image by extending them to the fuzzy case. Such an extension, called fuzzy geometry, includes the topological concepts of connectedness, adjacency and surroundedness, convexity, area, perimeter, compactness, height, width, diameter, extent, elongatedness, adjacency and degree of adjacency. These measures have been found to reflect the spatial (geometrical) ambiguity of an image and thus seem to be useful in providing soft decision for image description and analysis.

The present work is an attempt to demonstrate how the concept of fuzzy geometrical properties can be utilized in formulating image processing algorithms for providing both fuzzy and nonfuzzy (as a special case) outputs. It consists of two parts. In the first part some new properties namely, length, breadth, index of area coverge (IOAC), major axis, minor axis, center of gravity and density along with their definitions and illustrations are provided. The concepts of Rosenfeld's 'adjacency' and 'degree of adjacency' are critically examined and their new versions are defined. The second part consists of defining various algorithms for image segmentation and skeletonization. Segmentation again includes both gray level thresholding and pixel classification.

The measures involving spatial information are evaluated either in terms of the cooccurrence matrix or in terms of a local histogram computed over each row and each column. This in turn makes their conceptual realization easier and computation faster. It is to be mentioned here that these aspects did not get attention while developing the concepts by Rosenfeld.

Standard S [18] and Z functions are used for extracting the 'bright image' plane $\mu(X)$ from an image $X$ for its object extraction. The parameters compactness, IOAC and degree of adjacency are optimized for gray level thresholding. Adjacency measure and membership value of individual pixels computed over $\mu(X)$ are considered for pixel classification. For extracting the fuzzy skeleton of $X$, the measure compactness or IOAC is optimized on various $\alpha$-cuts. These $\alpha$-cuts are obtained from core line membership plane which is characterized by the

* At present, Dr. Pal is with the NASA Johnson Space Center, PT4/Software Technology Branch, Houston, TX 77058, USA.

gray level intensity, and the horizontal and vertical distances of the pixel from the fuzzy segmented $\varepsilon$-edges of $X$.

The effectiveness of the algorithms is demonstrated on various input images having wide range of histograms. The fuzzy outputs obtained are converted to their crisp (nonfuzzy) versions while comparing their performance with some of the recently developed algorithms [3, 5, 9].

## 2. Existing geometrical properties

A fuzzy subset of a set $S$ is a mapping $\mu$ from $S$ into $[0, 1]$. For any $p \in S$, $\mu(p)$ is called the degree of membership of $p$ in $\mu$. Supports of $\mu$ is an ordinary set and is defined as

$$S(\mu) = \{p \mid \mu(p) > 0\}.$$

$p$ is called a cross-over point of $\mu$ if $\mu(p) = 0.5$. A crisp (ordinary or nonfuzzy) subset of $S$ can be regarded as a special case of a fuzzy subset in which the mapping $\mu$ is into $\{0, 1\}$.

The various geometrical properties of $\mu$ as defined by Rosenfeld [14] are given below with illustration.

**Area:** The area of a fuzzy subset $\mu$ is defined as

$$a(\mu) = \int \mu \qquad (1)$$

where the integration is taken over a region outside which $\mu = 0$. For $\mu$ being piecewise constant (in case of digital image) the area is

$$a(\mu) = \sum \mu \qquad (2)$$

where the summation is over a region outside which $\mu = 0$. The area is therefore the weighted sum of the regions on which $\mu$ has constant value weighted by these values.

**Example 1.** Let $\mu$ be of the form

| | | |
|---|---|---|
| 0.2 | 0.4 | 0.3 |
| 0.2 | 0.7 | 0.6 |
| 0.6 | 0.5 | 0.6 |

Then area $a(\mu) = 4.1$.

**Perimeter:** If $\mu$ is piecewise constant, the perimeter of $\mu$ is defined as

$$p(\mu) = \sum_{i,j,k} |\mu(i) - \mu(j)| * |A(i, j, k)|. \qquad (3)$$

This is just the weighted sum of the lengths of the arcs $A(i, j, k)$ along which the regions having $\mu$ values $\mu(i)$ and $\mu(j)$ meet, weighted by the absolute difference of these values. In case of an image if we consider the pixels as piecewise constant regions, and the common arc length for adjacent pixels as unity then the perimeter of an image is defined by

$$p(\mu) = \sum_{i,j} |\mu(i) - \mu(j)| \qquad (4)$$

where $\mu(i)$ and $\mu(j)$ are the membership values of two adjacent pixels. For the fuzzy subset $\mu$ of Example 1, perimeter $p(\mu) = 2.3$.

**Compactness:** The compactness of a fuzzy set $\mu$ having area $a(\mu)$ and perimeter $p(\mu)$ is defined as

$$\text{comp}(\mu) = a(\mu)/p^2(\mu). \qquad (5)$$

Physically, compactness means the fraction of the maximum area (that can be encircled by the perimeter) actually occupied by the object. In the nonfuzzy case the value of compactness is maximum for a circle and this value is $\frac{1}{4}\pi$. In case of a fuzzy disc, where the membership value is only dependent on its distance from the center, this compactness value is $\geqslant \frac{1}{4}\pi$ [14]. Of all possible fuzzy discs compactness is therefore minimum for its crisp version. For the fuzzy subset $\mu$ of Example 1, comp$(\mu) = 0.775$.

**Height and width:** The height and width of a fuzzy set $\mu$ are defined as

$$h(\mu) = \int \max_x \{\mu(x, y)\} \, dy \qquad (6)$$

and

$$w(\mu) = \int \max_y \{\mu(x, y)\} \, dx \qquad (7)$$

where the integration is taken over a region outside which $\mu(x, y) = 0$. For a digital picture the definitions take the form

$$h(\mu) = \sum_y \max_x \{\mu(x, y)\} \qquad (8)$$

and

$$w(\mu) = \sum_x \max_y \{\mu(x, y)\}. \tag{9}$$

So, height/width of a digital picture is the sum of the maximum membership values of each row/column. For the fuzzy subset $\mu$ of Example 1, the height is

$$h(\mu) = 0.4 + 0.7 + 0.6 = 1.7$$

and the width is

$$w(\mu) = 0.6 + 0.7 + 0.6 = 1.9.$$

**Adjacency:** Let $\mu$ and $\Gamma$ be two piecewise constant fuzzy sets of $S$. Then we can partition $S$ into a finite number of bounded regions $B(i)$, meeting pairwise along arcs, on each of which both $\mu$ and $\Gamma$ are constant, say having values $\mu(i)$ and $\Gamma(j)$. Let $\mu$ and $\Gamma$ be disjoint; then on each $B(i)$, either $\mu = 0$ or $\Gamma = 0$. Let $A(i, j, k)$ be the $k$-th arc length along which $B(i)$ and $B(j)$ meet, and let this arc length be $|A(i, j, k)|$. Then the adjacency between $\mu$ and $\Gamma$ is defined as

$$a(\mu, \Gamma) = \sum_{i,j,k} \mu(i)\Gamma(j)\, |A(i, j, k)|. \tag{10}$$

Evidently, if $\mu$ and $\Gamma$ are crisp, $a(\mu, \Gamma)$ is just the total length of their common border. In the fuzzy case, each arc lenth is weighted by the product $\mu(i) * \Gamma(j)$. $a(\mu, \Gamma)$ is 1 only when both $\mu(i)$ and $\Gamma(j)$ are 1 (full adjacency), and it is small when either of them is small (i.e. either of them is weakly present). In case of a digital picture, the adjacency of a pixel to one of its neighbors is the product of its membership value with that of its corresponding neighbor. For the center pixel of Example 1, adjacency is 0.42 with its right neighbor.

**Degree of adjacency:** Intuitively two regions $S$ and $T$ in a digital picture are somewhat adjacent if some of the border pixels of $S$ touch (nearly) some of the border pixels of $T$; the degree of adjacency depends on how nearly they touch and along how much of their length they do so. Let $\mathrm{BP}(S)$ be the set of border pixels of $S$. Take any border pixel $p \in \mathrm{BP}(S)$. Let $d(p)$ be the shortest distance of this pixel $p$ from the border of $T$. Then the degree of adjacency between $S$ and $T$ is defined as

$$a(S, T) = \sum_{p \in \mathrm{BP}(S)} \frac{1}{1 + d(p)}. \tag{11}$$

## 3. New geometrical properties

In this section we will introduce some new fuzzy geometric properties of image subsets.

**Length:** The length of a fuzzy set $\mu$ is defined as

$$l(\mu) = \max_x \left\{ \int \mu(x, y)\, \mathrm{d}y \right\} \tag{12}$$

where the integration is taken over the region outside which $\mu(x, y) = 0$. In case of a digital picture the expression takes the form

$$l(\mu) = \max_x \left\{ \sum_y \mu(x, y) \right\}. \tag{13}$$

**Breadth:** The breadth of a fuzzy set $\mu$ is defined as

$$b(\mu) = \max_y \left\{ \int \mu(x, y)\, \mathrm{d}x \right\} \tag{14}$$

where the integration is taken over the region outside which $\mu(x, y) = 0$. In case of a digital picture,

$$b(\mu) = \max_y \left\{ \sum_x \mu(x, y) \right\}. \tag{15}$$

The length/breadth of an image fuzzy subset gives its longest expansion in the $Y$ direction/$X$ direction. If $\mu$ is crisp, $\mu(x, y) = 0$ or 1; then length/breadth is the maximum number of pixels in a column/row. Comparing equation (13) with (8) or (15) with (9) we notice that the length/breadth takes the summation of the entries in a column/row first and then maximizes over different columns/rows, whereas the height/width maximizes the entries in a column/row and then sums over different columns/rows. For the fuzzy subset $\mu$ in Example 1, $l(\mu) = 1.6$ and $b(\mu) = 1.7$.

**Index of area coverage (IOAC):** The index of area coverage of a fuzzy set may be defined as

$$\mathrm{IOAC}(\mu) = \frac{a(\mu)}{l(\mu)b(\mu)}. \tag{16}$$

In the nonfuzzy case, the IOAC has a value of 1 for a rectangle (placed along the axes of measurement). For a circle this value is $\pi r^2/(2r*2r)=\frac{1}{4}\pi$. IOAC of a fuzzy image represents the fraction (which may be improper also) of the maximum area (that can be covered by the length and breadth of the image) actually covered by the image.

For the fuzzy subset $\mu$ of Example 1, the maximum area that can be covered by its length and breadth is $1.6*1.7=2.72$, whereas the actual area is 4.1, so the IOAC $=4.1/2.72=1.51$. Note the difference between IOAC and comp($\mu$). Again, note the following relationships:

$$l(\mu)/h(\mu)\leq 1, \tag{17a}$$

$$b(\mu)/w(\mu)\leq 1. \tag{17b}$$

When equality holds for (17a) or (17b) the object is either vertically or horizontally oriented.

**Major axis:** Find the length of the object. Now rotate the axes through an angle $\theta$, $\theta$ varying between 0° and 90°. The angle for which length is maximum is said to be the angle of inclination of the object (with the vertical). The corresponding axis along which the length is maximum is said to be the major axis. The length along the major axis denotes the expansion of the object.

**Minor axis:** The axis perpendicular to major axis, for which breadth is maximum is defined as the minor axis of the object.

**Center of gravity:** The center of gravity (CG) of an object can be defined in various ways. Two such definitions are given here.

(a) The CG of an object can be defined as the point of intersection of the major and the minor axes.

(b) Take any pixel as the center. Take a neighborhood of radius $r$. Find the energy (area) of the circle. Now shift the center of the circle over all the pixels of the object. The center for which the energy is maximum is defined as the CG. If there is any tie then increase the radius and obtain the CG.

For the fuzzy subset $\mu$ of Example 1, length is $l(\mu)=1.6$ and breadth is $b(\mu)=1.7$. Now if we rotate the object by 45° then its length is $l(\mu)=0.6+0.7+0.6=1.9$.

Hence the object is inclined at an angle of 45° with the vertical axis. So by the minor axis of this image we mean the axis inclined at an angle of 45° with the vertical. Similarly the minor axis of this object is inclined at an angle of 45° with horizontal. Trivially the CG of this object is through the pixel having membership 0.7.

**Density:** The density of a fuzzy set $\mu$ having $N$ supports may be defined as

$$d(\mu)=\int \mu/N=a(\mu)/N. \tag{18a}$$

For a digital image characterized by $\mu$, its density is

$$d(\mu)=\sum_{i=1}^{N}\mu(i)/N. \tag{18b}$$

The maximum value of density is 1 and this value occurs only for a nonfuzzy case. Density can be used for finding the CG of an image. If we break the image into different regions then the region having the maximum density may be regarded to contain the CG.

**Adjacency:** The definition of adjacency given in (10) does not fully agree with our intuition. Let us take two piecewise constant regions $\mu$ and $\Gamma$. We say $\mu$ and $\Gamma$ are more adjacent if the difference of the membership value of $\mu$ and $\Gamma$ are less (whatever be their actual values). For example, let us take the membership values of the regions $\mu$ and $\Gamma$ as 0.2 and 0.25 respectively in the first case and 0.8 and 0.85 in the second case. Since the difference of the membership values is the same in both the cases their adjacency is also expected to be same (assuming the length of their common border to be the same). But according to (10) this value is 0.05 in the first case whereas 0.68 in the second case. One may, therefore, define adjacency as

$$a(\mu,\Gamma)=\sum_{i,j,k}\frac{|A(i,j,k)|}{1+|\mu(i)-\Gamma(j)|}. \tag{19}$$

Here the adjacency value is not dependent upon the absolute membership values of the regions, rather it is a function of the difference of their membership values. When $\mu(i)=\Gamma(j)$ and the length of the common boundary between the regions is unity the adjacency value is maximum (=1). The lesser the difference between $\mu$ and $\Gamma$, the more is the adjacency and vice versa.

**Degree of adjacency:** The definition of the degree of adjacency (11) given by Rosenfeld gives a measure of physical adjacency of two regions $S$ and $T$. It does not say anything about their membership values. In practice, it is reasonable to determine adjacency between two regions by their both physical and gray level distances. So the degree of adjacency can be defined as

$$a(S, T)=\sum_{p \in \mathrm{BP}(S)} \frac{1}{1+|\mu(p)-\Gamma(q)|} * \frac{1}{1+d(p)}. \tag{20}$$

Here $d(p)$ is the shortest distance between $p$ and $q$, $q$ is a border pixel of $T$ and $p$ is a border pixel of $S$. The other symbols have their same meaning as in the previous discussion. $a(S, T)$ denotes the degree to which the regions $S$ and $T$ are adjacent. The degree of adjacency of two regions is maximum (=1) only when they are physically adjacent, i.e. $d(p)=0$ and their membership values are also equal, i.e. $\mu(p)=\Gamma(q)$. If two regions are physically adjacent then their degree of adjacency is determined only by the difference of their membership values. Similarly, if the membership values of two regions are equal their degree of adjacency is determined by their physical distance only.

It is to be noted that when $d(p)=0$ for all $p$ (i.e. when $S$ is surrounded by $T$ or vice versa), $|A(i, j, k)|=1$ (because $p$ and $q$ are adjacent) and equation (20) reduces to (19).

**Example 2.** Let us consider a scene having two regions only (Figure 1). The gray levels of the regions in Figures 1(a) and (b) are identical but the regions in Figure 1(b) are closer to each other compared to Figure 1(a). So the degree of adjacency of the regions in Figure 1(b) should be more than that in Figure 1(a). In Figures 1(b) and (c) the relative positions of the regions are the same, but the difference of gray levels of the border pixels in Figure 1(b) is more than that in Figure 1(c). So from intuition we would expect

```
(a)                  9GKPSTVPNGDC78
                     9GJKSTVTVJCA88
                     96HJOVUMTRPHA8
                     9AJNSUVMKGA978
                     9GHKMSTVRPHCA8

     AS49HKOTTSNKGC8
     AFGKLPSUTPMJGF8
     AFSHSTVUJHCA998
     ADEGKOVSSJDA988
     AAHKRTMJFA89876
     ABJOSTTVUSKFGA8
     AAGHKUVRMHFC968
```

```
(b)   9GKPSTVPNGDC78
      9GJKSTVTVJCA88
      96HJOVUMTRPHA8
      9AJNSUVMKGA978
      9GHKMSTVRPHCA8

     AS49HKOTTSNKGC8
     AFGKLPSUTPMJGF8
     AFSHSTVUJHCA998
     ADEGKOVSSJDA988
     AAHKRTMJFA89876
     ABJOSTTVUSKFGA8
     AAGHKUVRMHFC968
```

```
(c)   9GKPSTVPNGDC78
      9GJKSTVTVJCA88
      96HJOVUMTRPHA8
      9AJNSUVMKGA978
      9HKPTSTMKFDCA8

     AS49HKOTTSNKGC8
     AFGKLPSUTPMJGF8
     AFSHSTVUJHCA998
     ADEGKOVSSJDA988
     AAHKRTMJFA89876
     ABJOSTTVUSKFGA8
     AAGHKUVRMHFC968
```

Fig. 1. (a) A scene with two regions. (b) Same as in (a), but the relative positions of the regions are different. (c) As in (b), but the gray levels of the border pixels of one region are different.

that the degree of adjacency of the regions in Figure 1(c) is more than that in Figure 1(b).

The $a(S, T)$ values computed with equation (20) are 0.062, 0.143 and 0.189 for Figures 1(a), (b) and (c) respectively. So the results agree well with our intuition.

In the following sections we will describe how these geometrical concepts can be incorporated in formulating various algorithms for gray level thresholding, pixel classification and skeletonization. For developing the algorithms we will be concentrating only on the parameters length, breadth, compactness, IOAC, adjacency and degree of adjacency.

## 4. Object extraction by degree of adjacency minimization

Equation (20) shows that, the higher the contrast (difference in gray levels) between two regions and greater the distance between them, the lower is their degree of adjacency. Therefore, a lower value of adjacency implies that the segments (clusters) formed are more valid (separable) considering both their gray level and physical distances. For this reason we will use minimization of degree of adjacency as a criterion for extracting segments of an image.

### *4.1 Formulation of algorithm* (Algorithm 1)

Let us consider an $L$-level digital image $X$ of size $M \times N$ and having gray level values from $l_{\min}$ to $l_{\max}$. Let the object pixels have gray level values $\leqslant s$ and the background pixels have gray level values $>s$, where $l_{\min} \leqslant s \leqslant l_{\max}$. In other words, we consider the regions object and background with respect to gray levels only. In such a case the degree of adjacency between the regions (object and background) is defined as (from equation 20)

$$a(O, B) = \sum_{i,j} \frac{1}{1 + |i - j|} * \frac{1}{1 + d} \tag{21}$$

where $i$ and $j$ represent the gray values of an object pixel and a background pixel respectively such that $j$ is a neighbor of $i$, and $d$ is the physical distance of the pixel having gray level $j$ from the pixel having gray level $i$.

Since we are considering only the border pixels (the transition between object and background) for computing the degree of adjacency between two regions (with respect to gray levels only), the physical distance of a border pixel of object region from that of background region is zero. So putting $d = 0$ in

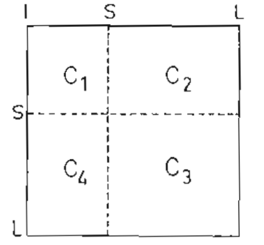

Fig. 2. Four submatrices (quadrants) of the cooccurrence matrix of an image.

equation (21) we get

$$a(O, B) = \sum_{i,j} \frac{1}{1 + |i - j|} \tag{22}$$

where $j$ is a neighbor of $i$. The information regarding $i$ and $j$ can be obtained from the coocurrence matrix of $X$.

**Cooccurrence matrix:** The cooccurrence matrix $C = [c(i, j)]$ of an $L$-level image is an $L \times L$ matrix such that $c(i, j)$ denotes the $(i, j)$-th entry of the matrix and gives the number of times the gray level $j$ follows the gray level $i$ (i.e. the gray level $j$ is a neighbor of the level $i$) in a specific fashion.

Now for a particular threshold $s$, the matrix $C$ may be divided into 4 parts namely $C_1$, $C_2$, $C_3$ and $C_4$ (Figure 2). Entries in $C_1$ and $C_3$ refer to the transitions within object and background respectively, whereas those in $C_2$ and $C_4$ correspond to transitions from object to background and vice versa.

So the entries in $C_1$ and $C_3$ contribute nothing to the degree of adjacency measure (22); only those of $C_2$ and $C_4$ will contribute. Equation (22) thus takes the form (considering $j$ as one of the four neighbors of $i$)

$$a(O, B) = \sum_{\substack{i,j \\ i \leqslant s \\ j > s}} \frac{c[i, j]}{1 + |i - j|} + \sum_{\substack{i,j \\ i > s \\ j \leqslant s}} \frac{c[i, j]}{1 + |i - j|}. \tag{23}$$

From (23) it is evident that the value of $a(O, B)$ is less when the difference of $i$ and $j$ is more and the corresponding $c[i, j]$ is less. In an image with increase in $|i - j|$, $c[i, j]$ usually decreases and the elements in $C$ thus correspond mainly to a low value of $|i - j|$. When $s$ corresponds to the appropriate boundary (threshold) between two

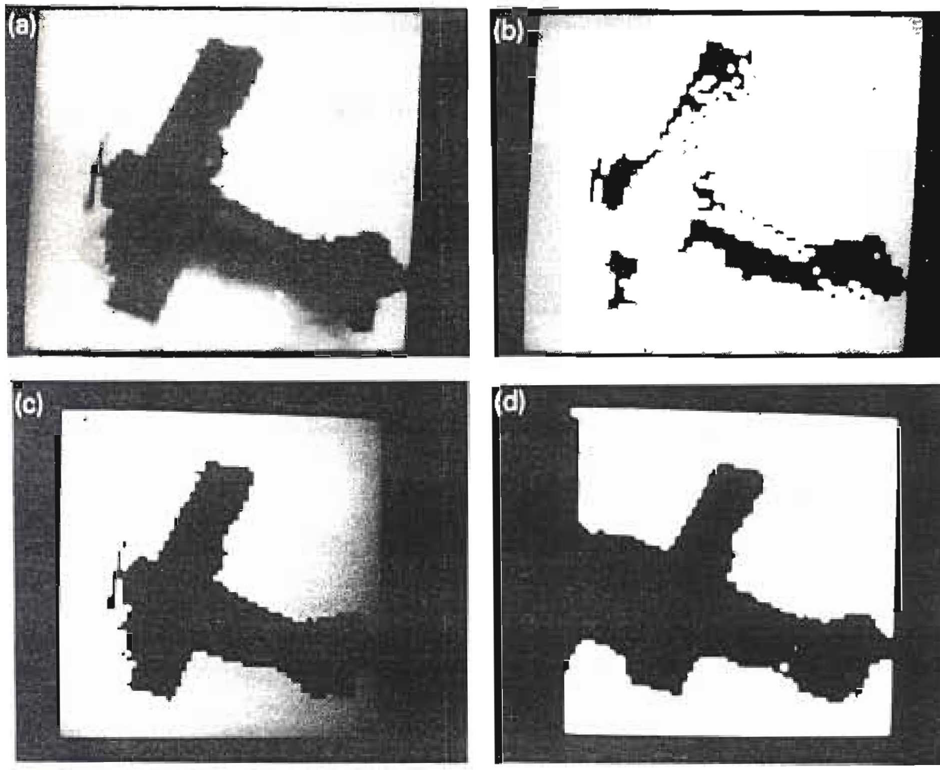


Fig. 3. Gray level thresholding of biplane image. (a) Input. (b) Threshold = 6. (c) Threshold = 14. (d) Threshold = 24.

regions, there will be a minimum number of pixel intensities having low $c[i, j]$ ($i \leq s$, $j > s$ or $i > s$, $j \leq s$) value; thus contributing least towards $a(O, B)$. This optimum (minimum) value of $a(O, B)$ would be greater for any other choice of $s$. The algorithm therefore consists of the following steps:

Step 1: Take a threshold $s$, say between $l_{min}$ and $l_{max}$.

Step 2: Calculate $a(O, B)$ using equation (23).

Step 3: Iterate steps 1 and 2 for different values of $s$; select that $s$ as an optimum threshold for which $a(O, B)$ is globally minimum.

### 4.2 Implementation and results

Three images are considered, namely, Biplane, Lincoln, and Blurred Chromosome [Figures 3(a), 4(a) and 5(a)]. The thresholds obtained by the algorithms are shown in Table 1. Some of the thresholded images are shown in

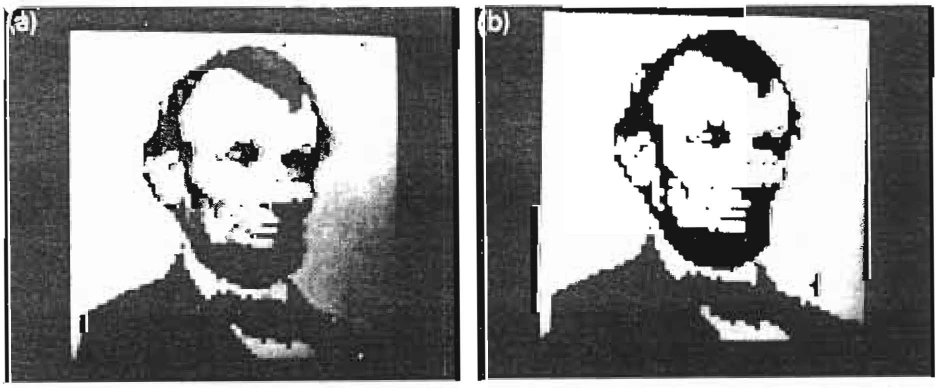


Fig. 4. Gray level thresholding of Lincoln image. (a) Input. (b) Threshold = 10.

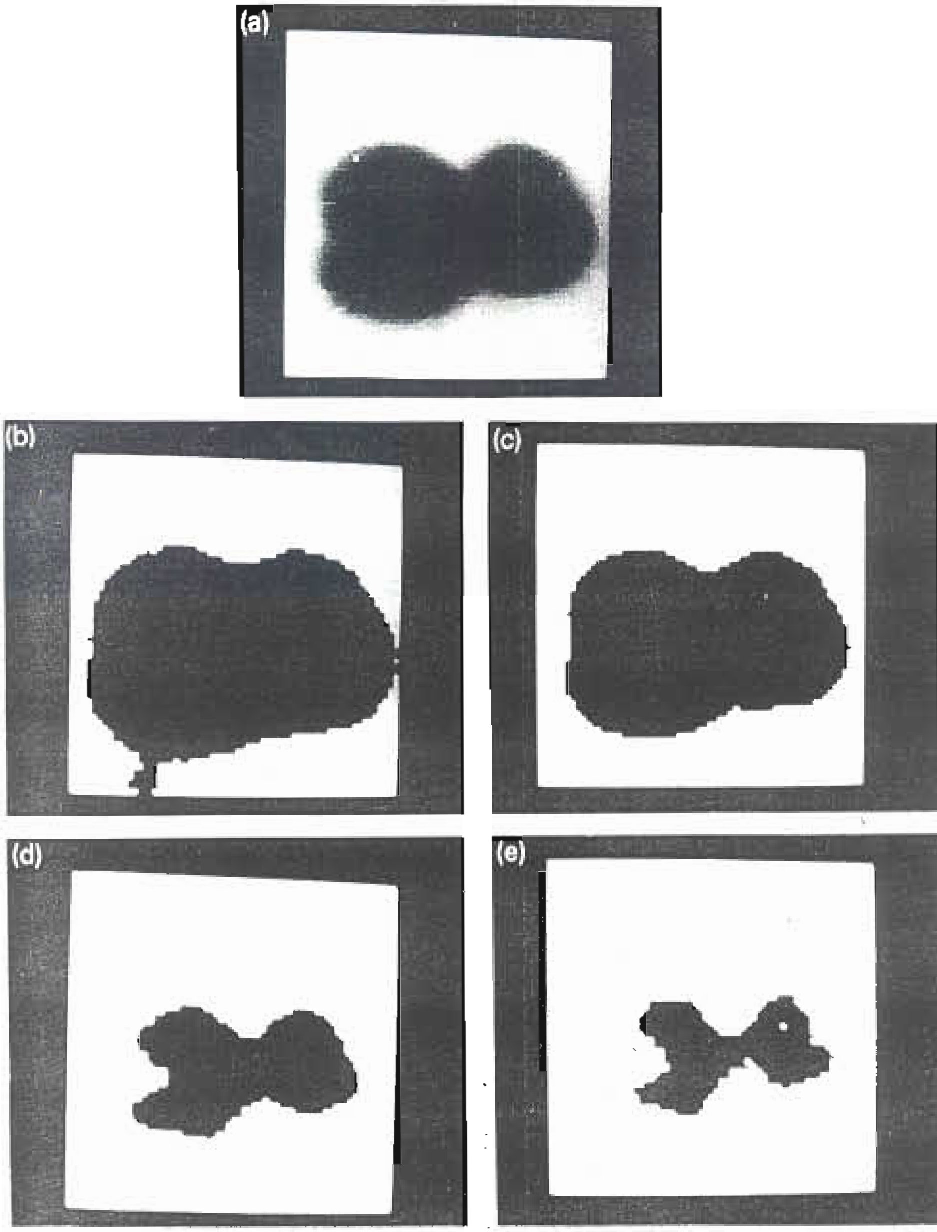


Fig. 5. Gray level thresholding of blurred chromosome image. (a) Input. (b) Threshold = 32. (c) Threshold = 40. (d) Threshold = 54. (e) Threshold = 56.

Table 1. Thresholds based on Algorithm 1

| Images | Degree of adjacency | Deg. of adj. + int. scatter |
|---|---|---|
| Biplane | 11* 14 22 | 11 14* 22 30 |
| Lincoln | 3 5 10* 13 18 24 | 6 10* 13 16 18 24 |
| Blurred chromosome | 19 22 30 38 40* 43 45 53 | 19 22 30 38 40* 43 |

* Global minima

Figures 3, 4 and 5 as a typical illustration. Since there is not much variation in global thresholds for the Lincoln image, only one thresholded version is shown here.

The results agree well with those of the recently developed algorithms based on cooccurrence matrix [5] and entropy measure [3]. Thresholds for Biplane, Lincoln and Blurred Chromosome were found to be 13, 10 and 42 respectively when conditional entropy was taken as a criterion [3].

An experiment was also done by including a measure called 'total internal scatter' (based on $C_1$ and $C_3$ of Figure 2) within object and background,

$$S(T) = S(O) + S(B) \tag{24}$$

where

$$S(O) = \sum_{\substack{i,j \\ i,j \le s}} |i - j|, \quad l_{\min} \le s \le l_{\max}, \tag{25}$$

$$S(B) = \sum_{\substack{i,j \\ i,j > s}} |i - j|, \tag{26}$$

as an additional criterion, but it did not seem to change (as seen from Table 1) the performance as obtained by (23) alone. This conforms well to the earlier findings of Pal and Pal [3] where the second order local entropy (based on $C_1$ and $C_3$) was found to be inferior to that of the conditional entropy (based on $C_2$ and $C_4$).

## 5. Object extraction by optimizing compactness and IOAC

### *5.1. Selection of membership function*

Most of the geometrical properties (of an image fuzzy subset) such as area, perimeter, length, breadth, etc. are dependent not only on the shape of the image, but also on the membership values. If the object pixels have higher gray levels we can select the standard $S$ function [18] to extract a 'bright image' plane. The $S$ function is defined as follows:

$$\begin{aligned} \mu(x) = S(x; a, b, c) & \\ = 0 & \quad \text{if } x \le a, \\ = 2[(x-a)/(c-a)]^2 & \quad \text{if } a \le x \le b, \\ = 1 - 2[(x-c)/(c-a)]^2 & \quad \text{if } b \le x \le c, \\ = 1 & \quad \text{if } c \le x, \end{aligned} \tag{27}$$

with cross-over point $b = \frac{1}{2}(a + c)$ and the window size $w = c - a$. Thus for a fixed cross-over point (say $b = s$, where the $\mu$ value is 0.5), pixels have gray levels $>s$ will have $\mu$-values $>0.5$ and pixels having gray levels $<s$ will have $\mu$-values $<0.5$.

On the other hand, when the object pixels have lower gray levels compared to background pixels, we would select a function complementary to the $S$-function (i.e. $(1 - S)$-function) which is called $Z$-function to represent a 'dark image' plane.

It is to be mentioned here that the criteria regarding the selection of membership functions along with the window size in image processing problems have recently been reported by Murthy and Pal [2]. The criteria involve symmetry in ambiguity around the cross over point and bound functions based on the properties of fuzzy correlation [1]. Zadeh's $S$-function (27) satisfies the aforesaid criteria.

### *5.2. Formulation of algorithm* (Algorithm 2)

It has been noticed in Sections 2 and 3 that for crisp sets the value of index of area coverage (IOAC) is maximum for a rectangle. Again, of all possible fuzzy rectangles IOAC is minimum for its crisp version. Similarly, in a nonfuzzy case the compactness is maximum for a circle and of all possible fuzzy discs compactness is minimum for its crisp version [14]. For this reason, we will use minimization (rather than maximization) of fuzzy compactness/IOAC as a criterion for image segmentation [6, 9, 16].

**Criteria for threshold selection.** Suppose we use equation (27) for obtaining the 'bright image' $\mu(X)$ of an image $X$. Then for a particular cross-over point selected at, say, $b = s$, the pixels having gray levels $>s$ will have $\mu$ values $>0.5$ and those having gray levels $<s$ will have $\mu$ values $<0.5$. This implies allocation of the gray levels into two regions. The terms comp($\mu$) and IOAC($\mu$) then reflect the average amount of ambiguity in the geometry (i.e. in spatial domain) of $X$. Therefore, modification of the cross-over point will result in different $\mu(X)$ planes (and hence different segmented versions), with varying amount of compactness or IOAC denoting fuzziness in the spatial domain. The $\mu(X)$ plane having minimum IOAC/compactness value can be regarded as an optimum fuzzy segmented version of $X$. This is optimum in the sense that for any other selection of cross-over point $b$, the value of compactness/IOAC will be greater.

For obtaining the nonfuzzy threshold one may take the cross-over point (which is considered to be the maximum ambiguous level) as the threshold between object and background. For images having multiple regions, one would have a set of such optimum $\mu(X)$ planes.

**Faster method of computation:** From Algorithm 2 it appears that one needs to scan an $L$-level image $L$ times (corresponding to $L$ cross-over points of the membership function) for computing the parameters for detecting its threshold. The time of computation can be reduced significantly by scanning it only once for computing its cooccurrence matrix, row histogram and column histogram, and by computing $\mu(l)$, $l = 1, 2, \ldots, L$, every time with the membership function of a particular cross over point.

Let $h(i)$, $i = 1, 2, \ldots, L$, be the number of occurrences of the level $i$, $c[i, j]$, $i = 1, 2, \ldots, L$, $j = 1, 2, \ldots, L$, the $(i, j)$-th entry of the cooccurrence matrix and $\mu(i)$, $i = 1, 2, \ldots, L$, the membership vector for a fixed cross over point of an $L$-Level image $X$. Then compute

$$a(X) = \sum_{i=1}^{L} h(i)\mu(i), \tag{28}$$

$$p(X) = \sum_{i=1}^{L} \sum_{j=1}^{L} c[i, j]\,|\mu(i) - \mu(j)|. \tag{29}$$

Let $R[m, l]$ represent the number of occurrences of the gray level $l$ in the $m$-th row of the image and $C[n, l]$ represent the number of occurrences of the gray level $l$ in the $n$-th column of the image. Then

$$l(X) = \max_{n} \sum_{l=1}^{L} C[n, l]\mu(l), \tag{30a}$$

$$b(X) = \max_{m} \sum_{l=1}^{L} R[m, l]\mu(l). \tag{30b}$$

### 5.3. Implementation and results

The algorithm has been implemented on the images of Biplane and Lincoln [Figures 3(a) and 4(a)] having black object and white background. Here $l_{min} = 1$ and $l_{max} = 32$. The different minima obtained by using Algorithm 2 (compactness and IOAC measures) for differeut window sizes are shown in Table 2.

The algorithm has also been implemented on two other images [Figures 6(a) and 5(a)] (viz., hand written characters 'Shu' and a Blurred Chromosome) with white object and black background. For the image 'Shu', $l_{min} = 1$ and $l_{max} = 32$, whereas for the blurred chromosome, $l_{min} = 13$ and $l_{max} = 60$. The different minima obtained by minimization of compactness and IOAC measures for different window sizes are shown in Table 3. Some of the crisp segmented versions of the 'Shu' image are shown in Figure 6.

Table 2. Thresholds based on Algorithm 2

| | Lincoln | | Biplane | |
|---|---|---|---|---|
| W | Comp | IOAC | Comp | IOAC |
| 6 | 10* | 11* 23 | 5* 14 27 | 11 19 24* |
| 8 | 10* | 11* 23 | 5* 26 | 11 19 24* |
| 10 | 10* | 11* 23 | 5* 26 | 12 24* |
| 12 | 10* | 11* 23 | 5* 24 | 13 24* |
| 14 | 9* | 11* 23 | 6* 23 | 13 24* |
| 16 | 9* | 11* | 6* 21 | 14 24* |

* Global minima.

The results (Tables 2 and 3) show that the thresholds (global) obtained by compactness measure, as expected, are very much worse for the 'Shu' image than that of the IOAC measure. This is because of the fact that the former attempts to make a circular approximation of the object for its extraction. As a result, some of the background portions get treated as object, thus failing to remove background noise. For the Biplane image, neither compactness nor IOAC has been able to provide a global threshold appropriate for its extraction. However, it is interesting to note that the appropriate thresholds 11–14 of the Biplane image came out as a local minimum only for the IOAC measure.

For a wide range of window sizes, the variation in global thresholds is seen to be insignificant. This corroborates the theoretical

Table 3. Thresholds based on Algorithm 2

| | Shu | | | Blurred chromosome | |
|---|---|---|---|---|---|
| W | Comp | IOAC | W | Comp | IOAC |
| 8 | 8* 24 | 8 12* | 8 | 33 56* | 30* 53 |
| 10 | 8* 24 | 9 12* | 12 | 33 56* | 30* 51 |
| 12 | 8* 23 | 9 13* | 16 | 55* | 31* 49 |
| 14 | 9* 23 | 13* | 20 | 54* | 32* 46 |
| 16 | 10* 22 | 14* | 24 | 52* | 34* |

* Global minima.

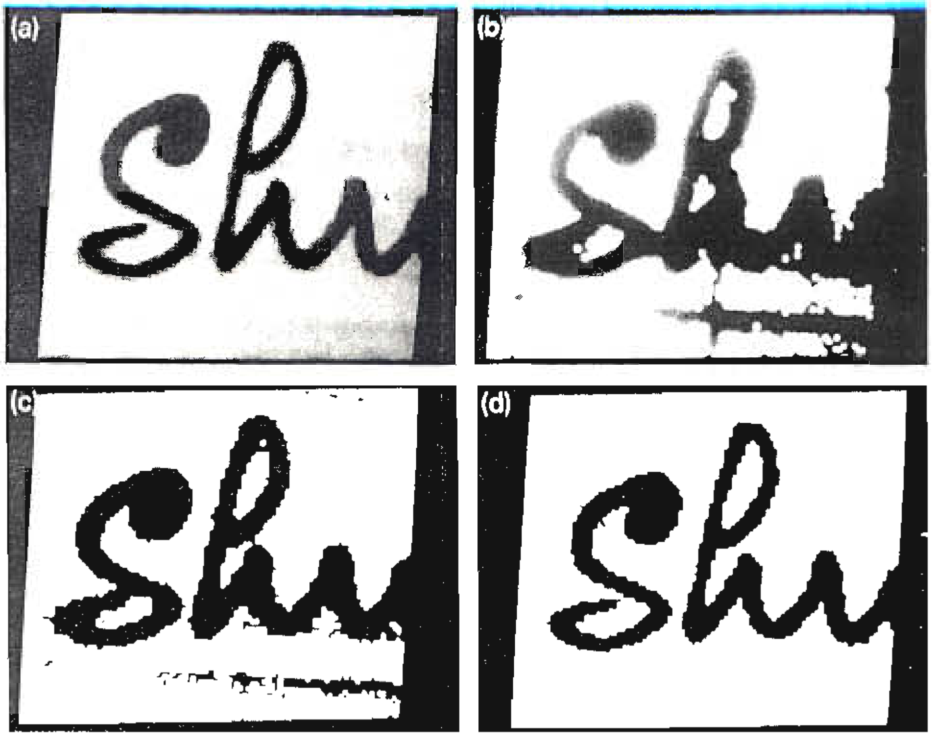


Fig. 6. Gray level thresholding of Shu image. (a) Input. (b) Threshold = 8. (c) Threshold = 10. (d) Threshold = 14.

findings of Murthy and Pal [2] and establishes further the flexibility of the fuzzy set theoretic approach. The overall performance of Algorithm 2 (considering the crisp version) is comparable to the very recently developed algorithm [3] based on local information and entropy measure.

It is to be noted here that the IOAC measure is dependent, to some extent, on the orientation of the object, If the object is along the horizontal and/or vertical direction, the measure will give good results. The result may be different if the object is inclined at an angle with the axes. In such cases one can rotate the axes and place it along the major and minor axes of the object.

The algorithm based on minimizing compactness measure was developed by Pal and Rosenfeld [9]. It has been included here only to compare its performance with that of the IOAC measure.

## 6. Pixel classification for object extraction

In Sections 4 and 5, algorithms for gray level thresholding have been described for object/background classification. Here we will explain a pixel classification algorithm for object/background separation based on adjacency measure (equation (10)).

### 6.1. Principle of pixel classification

A discussion on the choice of membership function is given in Section 5. The same discussion is also applicable here. The problem of pixel classification can be viewed as assigning the individual pixels into different types of classes depending upon the various features or properties possessed by the pixels with respect to those classes. An attempt is made here in classifying the pixels of a digital picture into two classes, namely object and background. The 'adjacency' (or the degree of belongingness) defined in (10) has been used as one of the features or criteria. In other words, the physical constraint that the intensity of a pixel is greatly influenced by its neighbor, has been exploited here for classification of pixels. The role of adjacency in this context is explained below.

Let $\mu(x, y)$ be the membership value denoting the degree of brightness of a pixel $p(x, y)$ or the degree of belongingness to the object region, say. The adjacency of a pixel to its neighbors can be defined as:

$$a(x, y) = \mu(x, y)\{\mu(x-1, y) + \mu(x+1, y) + \mu(x, y-1) + \mu(x, y+1)\}/4 \quad \text{(considering 4 neighbors)} \tag{31a}$$

$$= \mu(x, y)\left\{\left(\sum_{j=-1}^{j=+1}\sum_{i=-1}^{i=+1}\mu(x-i, y-j)\right) - \mu(x, y)\right\}\Big/8 \quad \text{(considering 8 neighbors).} \tag{31b}$$

If the higher gray levels represent the object region, then $a(x, y)$ is high if both $p(x, y)$ and its neighbors belong to the object, and it is low if both $p(x, y)$ and its neighbors belong to the background. $a(x, y)$ is medium if the pixel and its neighbors belong to object and background respectively or vice versa (i.e. the region corresponding to edge or boundary of the object). So $a(x, y)$ can be regarded as the degree of belongingness of the pixel $p(x, y)$ together with its neighbors to the object, say.

For classification of a pixel into object or background we consider $\mu(x, y)$ and $a(x, y)$ as two features. Keeping consistency in features, a pixel pattern can be represented as

$$p(x, y) = [a(x, y), \mu^2(x, y)]' \tag{31c}$$

in a two-dimensional feature space.

The pixel classification procedure can be thought of as a two-class minimum distance classifier [6] where the intial seed points or the representatives $S(1)$ and $S(2)$ of the two classes $C_1$ and $C_2$ (object and background) can be considered to be the two modes of the bivariate frequency distribution of the pattern vector $p(x, y)$. One may also consider [0, 0] and [1, 1] as the initial seed points, since these are the extreme points in the feature space belonging to object (background) and background (object). The algorithm developed using this concept is given below.

**Algorithm 3.**

Step 1: Choose the membership function, number of neighbours (4 or 8) for a pixel, and assign brightness/darkness membership value $\mu(x, y)$ to the pixel $p(x, y)$.

Step 2: Compute $a(x, y)$ using equation (31).

Step 3: Compute

$$d(i) = \|p(x, y) - S(i)\|, \quad i = 1, 2,$$

the distance of an unknown pixel vector $p(x, y)$ from the $i$-th seed point/representative vector of the classes.

Step 4: Assign the pixel $p(x, y)$ to $C_1$ if $d(1) < d(2)$ and to $C_2$ if $d(2) < d(1)$. Decide arbitrarily if $d(1) = d(2)$. (In such case a decision may also be taken by considering the number of neighbors of $p(x, y)$ belonging to object and background.)

Step 5: If $S(1)$ and $S(2)$ are chosen as the two modes, then STOP. If $S(1)$ and $S(2)$ are chosen as the two extreme points [0, 0] and [1, 1] then replace the seed points by the class means, and got to step 6.

Step 6: Iterate steps 2 to 5 until the difference between the seed points of two successive iterations is less than a prespecified small positive quantity ($\varepsilon$).

### 6.2. *Implementation and results*

Algorithm 3 has been implemented on the images of Biplane [Figure 3(a)], Lincoln [Figure 4(a)] and Chromosome [Figure 5(a)]. The results showing satisfactory partition are depicted in Figure 7. Here the initial seed points were taken as the extreme points [0, 0] and [1, I], and $\varepsilon = 0.001$. The basic advantage of Algorithm 3 is that it is not noise sensitive because, by taking the local information from the neighbors through $a(x, y)$, it attempts to reduce the effect of noise on classification. To demonstrate this, the algorithm has also been tested by adding noise to the image of Biplane. The noisy input images ($\sigma = 3$ and 5 with $\mu = 0$) are shown in Figure 8. The partitioned images are shown in Figures 9(a) and (b) respectively. The corresponding gray level thresholded images obtained by Algorithm 1 are also included here for comparison [Figures 9(c) and (d)].

## 7. Some comments on various object extraction algorithms

In Sections 4–6 we have described three different algorithms illustrating the way of

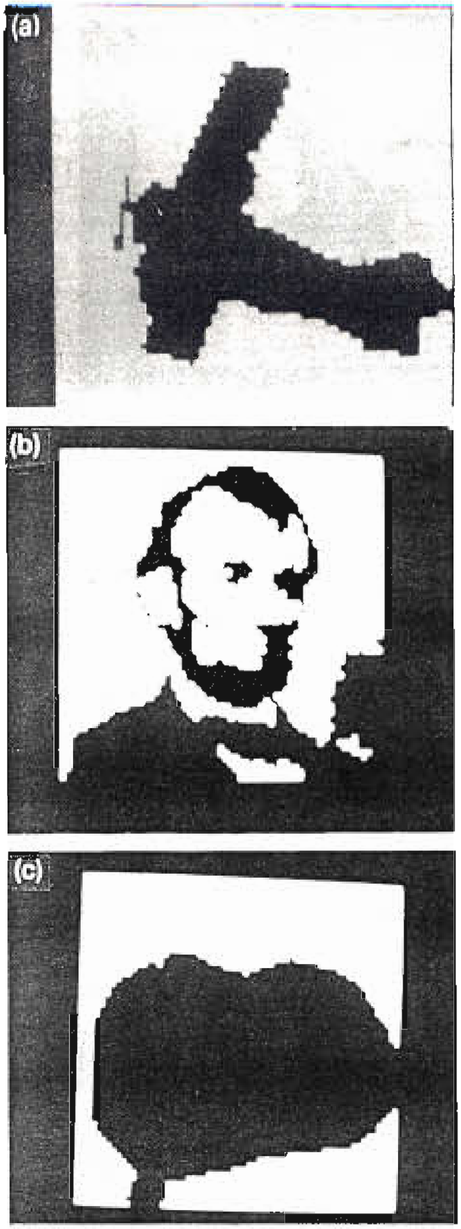


Fig. 7. Pixel classifications; (a) Extracted object pixels of Biplane. (b) Extracted object pixels of Lincoln. (c) Extracted object pixels of Blurred Chromosome.

implementing the concept of fuzzy geometry for object and background separation. The first two algorithms describe gray level thresholding, whereas the third one deals with a pixel classification technique.

Algorithm 1 optimizes the degree of adjacency between two regions (with respect to gray levels only) to find out the thresholds. This measure takes spatial information into account and is influenced by the quadrants $C_2$ and $C_4$ (Figure 2) of the cooccurrence of the gray levels. The algorithm is computationally faster and can be applied to any kind of image.

Algorithm 2 optimizes compactness/IOAC of the object region in an image. The algorithm is based on local information and takes the shape of the object into consideration. The compactness measure is partly dependent on the cooccurrence of the gray levels. Compactness optimization is expected to work better for circular compact objects, whereas the IOAC optimization gives good results for rectangular compact objects. The choice of window size does not seem to be very critical as long as it is restricted by the bound functions of Murthy and Pal [2]. This supports the theoretical findings in [2] and establishes the flexibility of the algorithms. Since IOAC does not require the calculation of cooccurrence of the level, it takes less time compared to compactness calculation.

The third algorithm describes another way of object extraction (region growing). The algorithm is based on both local and global information and is very much influenced by the neighbors of the pixels. The process is iterative, but converges very fast. Compared to the other two algorithms it is computationally less efficient but very less sensitive to noise.

## 8. Gray level image thinning

This section describes another application of compactness/IOAC measure for skeleton extraction of a gray level image. The output skeletons, as expected, are fuzzy in nature denoting the degree of belongingness of the pixels to the skeleton (core line). An optimum version has been obtained by computing the compactness/IOAC value on various $\alpha$-cuts $(1 > \alpha > 0)$ of the fuzzy skeleton plane. For extracting a single pixel width crisp version, one may retain only the highest valued pixels preserving connectivity among them.

### *8.1. Choice of membership function*

Given a fuzzy segmented version of an image (as described in Section 5), first of all assign a membership value to each pixel denoting its

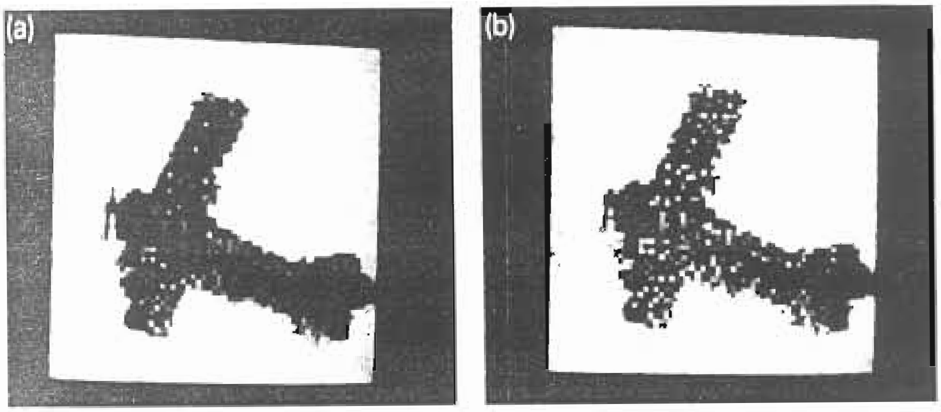


Fig. 8. Noisy biplane image. (a) $\mu = 0$, $\sigma = 3$, (b) $\mu = 0$, $\sigma = 5$.

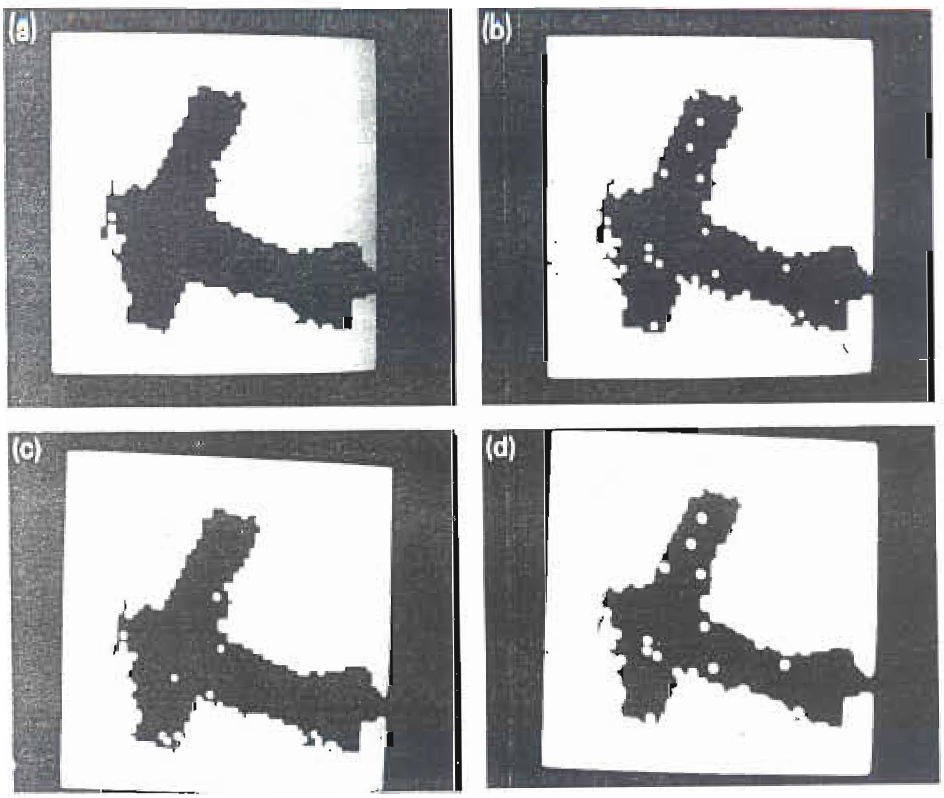


Fig. 9. Pixel classification and gray level thresholding of noisy biplane image. (a) Extracted object pixels of Figure 8(a) with Algorithm 3. (b) Extracted object pixels of Figure 8(b) with Algorithm 3. (c) Thresholded object of Figure 8(a) with Algorithm 1. Thresholded object of Figure 8(b) with Algorithm 1.

degree of belongingness to the skeleton (core line) of the object. The membership value is determined by three factors. These include the property of possessing maximum intensity, occupying vertically and horizontally middle positions from the $\varepsilon$-edges (pixels beyond which the membership value in the fuzzy segmented image becomes less than or equal to $\varepsilon$, $\varepsilon > 0$) of the object. It is to be noted that one may also consider here adjacency (equation (10)) as an additional feature which takes local information into account.

Let $x_{max}$ be the maximum pixel intensity in the image and $p(x_{mn})$ be the function which assigns the degree of brightness to the $(m, n)$-th pixel. Then the simplest way to define $p(x_{mn})$ is

$$p(x_{mn}) = x_{mn}/x_{max}. \tag{32a}$$

It is to be mentioned here that one may use other monotonically nondecreasing functions including the standard S-function (equation (27)) to define $p(x)$ with the flexibility of varying cross-over point. Equation (32a) is the simplest one with fixed cross-over point at $\frac{1}{2}x_{max}$.

Let $h_1$ and $h_2$ be the distances of the pixel $x_{mn}$ from its left and right $\varepsilon$-edges respectively (the distance being measured by the number of pixels separating the pixel under consideration from the $\varepsilon$-edge along that direction). Then $h(x_{mn})$ denoting the degree of occupying the horizontal central position in the object by the $(m, n)$-th pixel is defined as

$$\begin{aligned} h(x_{mn}) &= h_1/h_2 \quad \text{if } d(h_1, h_2) \leq 1 \text{ and } h_1 \leq h_2, \\ &= h_2/h_1 \quad \text{if } d(h_1, h_2) \leq 1 \text{ and } h_2 < h_1, \\ &= 2h_1/h_2(h_1 + h_2) \\ &\qquad\qquad \text{if } d(h_1, h_2) > 1 \text{ and } h_1 \leq h_2, \\ &= 2h_2/h_1(h_1 + h_2) \\ &\qquad\qquad \text{if } d(h_1, h_2) > 1 \text{ and } h_2 < h_1, \end{aligned} \tag{32b}$$

where $d(h_1, h_2) = |h_1 - h_2|$. If the vertical distances of a pixel from its top and bottom $\varepsilon$-edges are $v_1$ and $v_2$ respectively then its vertical membership function $v(x_{mn})$ can be defined similarly.

The two functions $h(x_{mn})$ and $v(x_{mn})$ assign higher membership values ($\approx 1.0$) to pixels towards the core of the image, whereas low membership values to pixels towards the edge. The term $h_1 + h_2$ or $v_1 + v_2$ in the denominator takes the extent of the object into consideration so that there is an appreciable amount of change in property value for the pixels away from the core.

These primary membership functions $p(x)$, $h(x)$ and $v(x)$ can then be combined in different ways to define $\mu_c(x_{mn})$ denoting the degree of belongingness of the pixel to the core line of the object. Two types of combination are described below.

*Weighted averaged method*:

$$\mu_c(x_{mn}) = w_1 h(x_{mn}) + w_2 v(x_{mn}) + w_3 p(x_{mn}), \tag{33a}$$

where $w_1 + w_2 + w_3 = 1$, with $w_1$, $w_2$, $w_3$ the weights attributed to the different primary membership functions. Usually one can consider the weight $w_3$ attributed to $p(x)$ to be higher and $w_1 = w_2$.

*Min–max method*:

$$\begin{aligned} \mu_c(x_{mn}) = \max\{&\min(h(x_{mn}), v(x_{mn})), \\ &\min(v(x_{mn}), p(x_{mn})), \\ &\min(p(x_{mn}), h(x_{mn}))\}. \end{aligned} \tag{33b}$$

Equation (33b) is chosen in such a manner that a pixel possesses higher $\mu_c$ value if two of its primary membership values are higher.

Equation (33) extracts (using both gray level and spatial information) the subset 'core line' such that the $\mu_c$ value of a pixel decreases as it moves towards the edge of the object region.

### *8.2. Optimum α-cut and skeleton extraction*

Having the $\mu_c(x_{mn})$ plane developed in the previous stage the optimum (in the sense of minimizing ambiguity in geometry or in the spatial domain) skeleton can be extracted from one of its $\alpha$-cuts having minimum comp($\mu$) or IOAC($\mu$) value. The $\alpha$-cut of $\mu_c(x_{mn})$ is defined as

$$\mu_c(\alpha) = \{x_{mn} \in X \mid \mu_c(x_{mn}) \geq \alpha\}, \quad 0 < \alpha < 1. \tag{34}$$

Modification of $\alpha$ will therefore result in different fuzzy skeleton planes with varying comp($\mu$) value. As $\alpha$ increases, comp($\mu$) initially decreases to a certain minimum and then for a further increase of $\alpha$, it increases. The initial decrease in comp($\mu$) can be explained by observing that for every value of $\alpha$, the border pixels having $\mu$-values less than $\alpha$ are not taken into consideration. So both area (equation (2)) and perimeter (equation (4)) are less than those for the previous value of $\alpha$. But the decrease in area is more than the decrease in its perimeter and hence the compactness (equation (5)) decreases (initially) to a certain minimum corresponding to a value of $\alpha = \alpha'$, say.

Further increase in $\alpha$ results in a $\mu_c(\alpha)$ plane consisting of a number of disconnected regions (because the majority of the core line pixels are dropped out). As a result, decrease in perimeter

Table 4. Optimum $\alpha$-cuts based on Algorithm 4

| | IOAC optimization | | Comp optimization | |
|---|---|---|---|---|
| Images | Weighted average | Min–Max | Weighted average | Min–Max |
| Shu | 0.563 | 0.625 | 0.563 | 0.406 |
| Biplane | 0.375 | 0.844 | 0.438 | 0.469 |

here is more than that of area and hence compactness increases. The $\mu_c(\alpha')$ plane having minimum compactness value can be taken as an optimum fuzzy skeleton version of the image $X$. This is optimum in the sense that for any other skeleton of $\alpha$ (i.e. $\alpha \neq \alpha'$), comp($\mu$) value would be greater. Similar is the case for IOAC measure.

$\mu_c(\alpha')$ can thus be regarded as a subset denoting the fuzzy skeleton of the image $X$. It is least compact (occupies smaller fractional area) or more crisp and has minimum spatial fuzziness as far as its core line extraction is concerned. If a nonfuzzy (or crisp) single pixel width skeleton is deserved, it can be obtained by a contour tracing algorithm [7, 17] which takes into account the direction of contour.

### 8.3. Implementation and results

Table 4 shows the optimum $\alpha$ values for the images of biplane and Shu corresponding to IOAC and compactness neasures and different methods. As a typical illustration, the skeletons only for compactness measure ($\varepsilon = 0.2$) are included in Figure 10. Again, to demonstrate the variation of compactness measure with $\alpha$ value, a graph is shown in Figure 11 for the image of Shu.

It is to be mentioned here that the use of the concept of $\varepsilon$-edge for obtaining $h(x_{mn})$ and $v(x_{mn})$ makes it appropriate and also meaningful instead of considering the crisp (hard) edge (i.e. $\varepsilon = 0$) as taken in the previous work [4] based on compactness measure only. Again, the variation of IOAC/compactness measure considering $\varepsilon$ (>0) edge, as expected, is seen to be smooth as compared to the case when $\varepsilon = 0$. The optimum $\alpha$-cuts (Table 4) obtained by IOAC and compactness measures do not seem to be much different.

## 9. Discussion and conclusions

An attempt has been made here to demonstrate the way of implementing the concept of fuzzy geometry in image processing/analysis problems for providing a soft decision. Some new measures have also been defined in this context. Various algorithms based on different geometrical measures are developed and are used to determine thresholds for object/background classification and skeleton extraction (both fuzzy and nonfuzzy).

The measures compactness, IOAC, adjacency and degree of adjacency mainly take local information into account. The key features (i.e. sensitivity to noise, shape and computational time) of the algorithms together with their types of applicability have been explained. The crisp

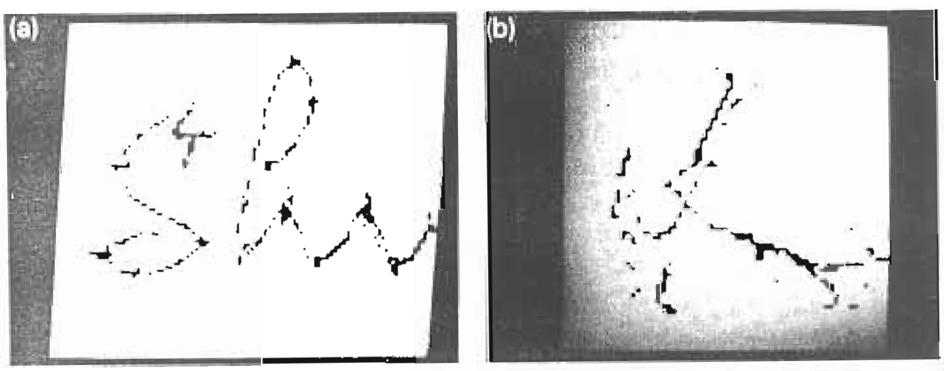


Fig. 10. (a) Extracted skeleton of the Shu image with equation (33a) and compactness measure. (b) Extracted skeleton of the Biplane image with equation (33a) and compactness measure.

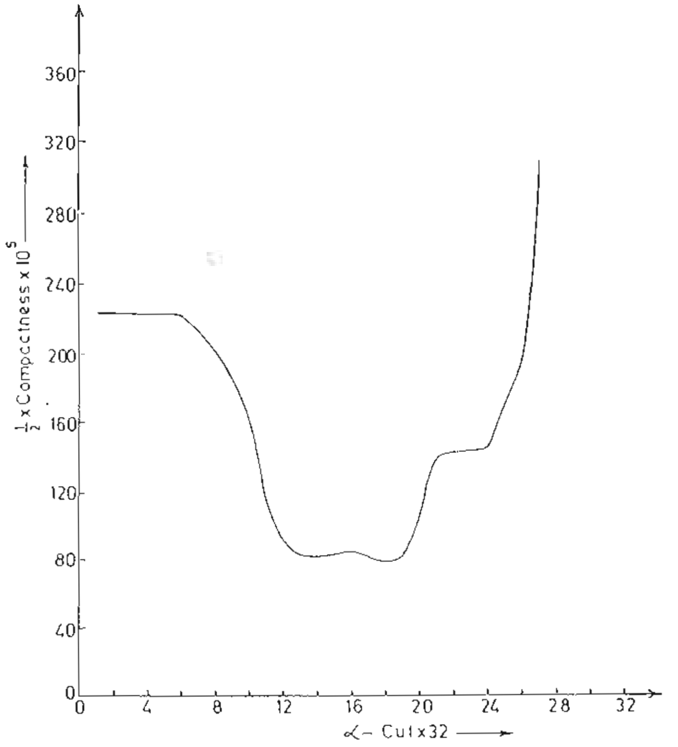


Fig. 11. Variation of compactness measure with $\alpha$-cuts (when equation (33a) is used).

output of the proposed algorithms are found to agree well with those of the conventional techniques recently developed using the cooccurrence matrix [3, 5]. The effect of window size of membership function is found to corroborate the earlier theoretical findings [2] showing the flexibility of Algorithm 2.

The application of major and minor axes, center of gravity and density is not considered here. Their definitions are introductory and may be further investigated.

It is to be mentioned here that the concept of fuzzy sets is more cumbersome to represent, and their properties are somewhat more expensive to compute. But as the computer memory and computing power are becoming cheaper, the fuzzy geometric approach to image analysis and description seems to deserve more serious considerations.

## Acknowledgment

The authors gratefully acknowledge Mr. S. Chakraborty for drawing the diagrams.

## References

[1] C.A. Murthy, S.K. Pal and D. Dutta Majumder, Correlation between two fuzzy membership functions, *Fuzzy Sets and Systems* 7 (1985) 23–38.

[2] C.A. Murthy and S.K. Pal, Histogram thresholding by minimizing gray level fuzziness, *Information Sciences* **60** (1992) 107–135.

[3] N.R. Pal and S.K. Pal, Entropic thresholding, *Signal Processing* **16** (1989) 97–108.

[4] S.K. Pal, Fuzzy skeletonization of an image, *Pattern Recognition Lett.* **10** (1989) 17–23.

[5] S.K. Pal and N.R. Pal, Segmentation based on measure of contrast, homogeneity and region size, *IEEE Trans. Systems Man Cybernet.* **17** (1987) 857–868.

[6] S.K. Pal and D. Dutta Majumder, *Fuzzy Mathematical Approach to Pattern Recognition* (John Wiley/Halsted Press), New York, 1986).

[7] S.K. Pal, R.A. King and A.A. Hashim, Image description and primitive extraction using fuzzy sets, *IEEE Trans. Systems Man Cybernet.* **13** (1983) 94–100.

[8] S.K. Pal, R.A. King and A.A. Hashim, Automatic gray level thresholding through index of fuzziness, *Pattern Recognition Lett.* **1** (1983) 141–146.

[9] S.K. Pal and A. Rosenfeld, Image enhancement and thresholding by optimizing fuzzy compactness, *Pattern Recognition Lett.* **7** (1988) 77–86.

[10] J.M.S. Prewitt, Object enhancement and extraction, in: B.S. Lipkin and A. Rosenfeld, Eds., *Picture Processing*

*and Psychopictorics* (Academic Press, New York, 1970) 75–149.

[11] A. Rosenfeld, Fuzzy digital topology, *Inform. and Control* 40 (1979) 76–87.

[12] A. Rosenfeld, On connectivity properties of grayscale pictures, *Pattern Recognition* 16 (1983) 47–50.

[13] A. Rosenfeld, The diameter of a fuzzy set, *Fuzzy Sets and Systems* 13 (1984) 241–246.

[14] A. Rosenfeld, Fuzzy geometry of image subsets, *Pattern Recognition Lett.* 2 (1984) 311–317.

[15] A. Rosenfeld and S. Haber, The perimeter of a fuzzy set, *Pattern Recognition* **18** (1985) 125–130.

[16] A. Rosenfeld and A.C. Kak, *Digital Picture Processing* (Academic Press, New York, 1982).

[17] A. Rosenfeld and R. Klette, Degree of adjacency or surroundedness, Technical Report, Center for Automation Research, University of Maryland, CAS TR-53, CS-TR-1380, 1984.

[18] L.A. Zadeh, Calculus of fuzzy restrictions, in: L.A. Zadeh, et al., Eds., *Fuzzy Sets and Their Application to Cognitive and Decision Process* (Academic Press, London, 1975) 1–39.